



Tradeoff between mass sensitivity and performance in quasi-zero stiffness vibration isolators

Paul Gilmore¹, Umesh Gandhi
Toyota Research Institute of North America
1555 Woodridge Ave
Ann Arbor, MI 48105
USA

S M Syed Abubakar Shaihan, Ramsharan Rangarajan
Mechanical Engineering, Indian Institute of Science Bangalore
CV Raman Rd
Bengaluru, Karnataka 560012
India

ABSTRACT

Quasi-zero stiffness isolators are a promising technology to reduce vibration transmission over a large frequency range while maintaining passive operation and low cost. Many different types of QZS isolators have been demonstrated utilizing a variety of mechanical, pneumatic, and magnetic components. While some of these types have their own unique challenges, other challenges are more general. Two of these challenges are mass sensitivity and hysteresis in the load-deflection curve caused by snap-through buckling, friction, or structural damping. This work investigates the impact of force-deflection hysteresis on isolation performance through experimental techniques. Results show that increasing hysteresis reduces the mass sensitivity but worsens the isolation performance at low frequencies. A tradeoff must be made between these two aspects but can be overcome by shifting the QZS region to different forces. A simple method to achieve this adaptability exists for certain types of QZS structures, therefore enable a variety of practical applications within a certain design window.

1. INTRODUCTION

Quasi-zero stiffness (QZS) isolators, otherwise known as high static, low dynamic stiffness (HSLDS) elements are structures which have nonlinear stiffness. Typically, there is a large positive stiffness at low deflection, zero stiffness at intermediate deflection, and high stiffness at large deflection. In a

¹paul.gilmore@toyota.com

vertical isolation system, the object of interest is placed on top of the isolator, and its weight should be such that the static equilibrium point is in the middle of the zero stiffness region. Zero stiffness around the operating point theoretically leads to natural frequency of zero and isolation over infinite frequency range. A large initial stiffness is needed to both create good load bearing capability and minimize the static deflection, and as a result HSLDS devices can avoid the tradeoffs associated with a linear isolator. This concept of using HSLDS structures to reduce vibration transmission is well known, and many different QZS structure designs have been proposed [1–3].

Despite good performance in theory, QZS isolators must overcome several challenges for practical applications. Some of these include overall isolator footprint and height, integration with the object using linear bearings, linkages, or other mechanisms which may affect the performance, variability of base vibration input direction, total stroke of the QZS region, and object weight variability. Another important parameter which may guide design choices is the target weight range of the object to be isolated. For example, certain QZS structures may be more suitable for small weights (20-100 N) while others may be more appropriate for larger weights (10^2 to 10^3 N and above). Throughout our investigations, we have found that a QZS isolator made from a compression spring and spring steel arch is suitable in the weight range of 20-100 N. At these forces, it can be made with relatively small footprint and small height while also having large stroke.

Another advantage the proposed structure is that the force-deflection hysteresis is very low. We have found that hysteresis due to friction is neglected in most studies on QZS isolators, yet hysteresis is often both difficult to avoid in practical devices, especially when weight is small, and has significant effect on the performance. Hysteresis may arise from friction in the isolator itself or support structures around it such as linear bearings, pins, and linkages. Having a negligible hysteresis in the isolator itself provides a good starting point upon which to minimize the overall hysteresis in a complete, packaged device.

On the other hand, our studies have shown that decreasing hysteresis also leads to much higher weight sensitivity. An isolator with no hysteresis may have impressive performance for a precise weight, but any variation in that weight will significantly increase the vibration transmission at low frequencies. At the same time, we have observed that isolators with higher hysteresis can maintain better performance when the weight varies by a certain percent. Several studies on effect of mistuned mass have been published but do not account for the effect of hysteresis [4–6]. A complete interpretation of the results is therefore not possible without knowledge of the hysteresis characteristics. The goal of this paper is to quantify the tradeoff between performance and weight sensitivity, allowing for more intelligent design decisions in targeted applications.

Lastly, the tradeoff can be avoided by being able to adjust the QZS force depending on the object weight. A simple method to accomplish this exists for certain types of QZS structures and will be demonstrated in this paper.

2. DESIGN AND MODELING OF QZS ISOLATOR

Most QZS isolators are realized using a positive stiffness spring in parallel with a negative stiffness element. If the negative stiffness element has a negative slope equal in magnitude to the positive spring slope, then QZS behavior is achieved. A QZS isolator using a compression spring as the positive stiffness element and a spring steel arch as the negative stiffness element is introduced in Figure 1. This QZS isolator has small force-deflection hysteresis which is due to the good elasticity of spring steel, minimal number of components, absense of mechanical joints, and absense of sliding contact surfaces.

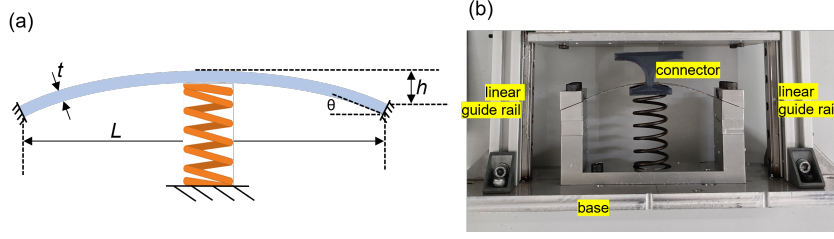


Figure 1: Design of QZS isolator using a spring steel prestressed arch: schematic with geometry (a), and fabricated prototype for testing (b).

Buckled beams and arches have been used previously as negative stiffness elements for QZS isolators [7–11]. These components are made with varying arrangements, boundary conditions, and materials. Modeling and design of buckled beams and arches subject to a transverse load have been reported [12, 13]. In this work, we propose the novel combination of a prestressed arch and clamped boundary conditions with non-zero clamp angle. Spring steel provides low structural damping, and the pre-stressed condition allows for simple assembly using off-the-shelf, flat spring steel stock. A CAE model of the spring steel arch created in Abaqus helped design the QZS isolator for a target weight of 40–50 N.

Table 1 lists the arch geometric parameters corresponding with Figure 1a. The unbuckled length is 110 mm, which results in a height of 11 mm post-buckling. The arch has clamped-clamped boundary conditions inclined at 20°. Clamped conditions eliminate the need for pin joints which add complexity and can potentially contribute to hysteresis. The 20 degree incline angle causes the beam force-deflection curve to be asymmetric, and therefore, although the arch is still bi-stable, the second stable point of the arch does not lie in the QZS region. This characteristic has the benefit that the load bearing is shared between the negative and positive stiffness elements [14]. A negative stiffness element with similar design was investigated by Zhang et al, but there were a few notable differences. The beam material was Nylon, it was fabricated without prestress, and the hysteresis was not considered [11]. Lastly, the connector shown in Figure 1b ensures that the arch snap-through motion is symmetric by constraining the center of the arch to have zero slope.

Table 1: Geometry of spring steel arch.

Geometric Parameter	L	w	t	h	θ
Value	98 mm	14 mm	0.35 mm	11 mm	20°

The isolator is subject to base excitation x_b according to the setup pictured in Figure 2a. The equation of motion of the mass m can be written as:

$$m\ddot{x}_m - f_{QZS}(x_b - x_m + x_o) + F_{fr}\text{sgn}(\dot{x}_m - \dot{x}_b) = -mg \quad (1)$$

where f_{QZS} is the force in the QZS isolator, x_o is the initial compression of the QZS isolator at static equilibrium, and F_{fr} is the friction force which gives rise to the hysteresis. The mass displacement x_m is defined to be zero at the static equilibrium position, x_o . At static equilibrium, Equation 1 then reduces to:

$$f_{QZS}(x_o) = mg \quad (2)$$

which can be solved numerically for x_o . We expect friction to be the dominant damping mechanism in this system and therefore assumed viscous and structural damping can be ignored. Since development of an analytical model for the arch was not a goal of this paper, the function f_{QZS} was chosen to be a third order polynomial fitted to the experimental force-deflection data. The fit was good within the QZS region and up until 2-3 mm outside the QZS region on either side (Figure 2b). Both the experimental measurements and model showed that the system always operated within this range and therefore the polynomial fit was a reasonable approximation. Equation 1 was solved numerically using 4th order Runge-Kutta method.

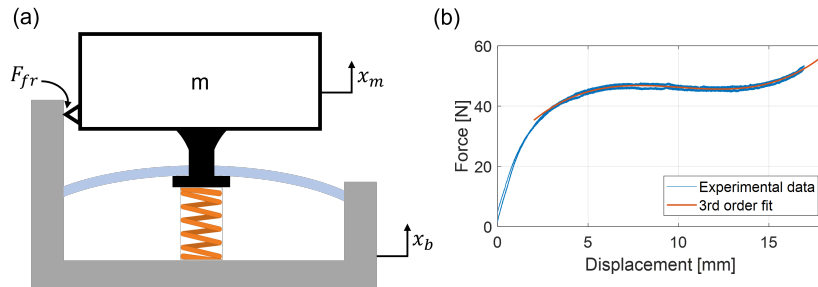


Figure 2: Base excitation setup used to evaluate the performance of the QZS isolator (a), and 3rd order polynomial fit of force-deflection data in QZS region (b).

3. DESIGN OF EXPERIMENTAL SETUP

We designed a mechanism to precisely control the friction force in the isolator in order to achieve the objectives of this paper. Without any modification, the isolator has about 1 N hysteresis in the QZS region. Our target was to control the hysteresis with a precision of 0.5 N and range of 8 N. The QZS isolator was modified with two sliding contact surfaces as shown in Figure 3a,b., one fixed to the base and one fixed to the mass. The surface fixed to the base is made from acetal and can also move horizontally on a linear guide system. The friction force between the two surfaces is controlled by preloading the acetal surface with a spring in the horizontal direction. A combination of acetal surface, spring constant of 2.89 N/mm, and spring length of 0.875 inches gave good sensitivity to control the friction force.

Interestingly, a similar experimental setup was developed by Liu et al to apply a friction force to a QZS isolator, but the friction force was not tunable and the mass sensitivity was not investigated. A conclusion of the study was that Coulomb friction could significantly decrease the resonant peak at the expense of small increases in transmissibility after resonance [15]. Here, the goal is to extend the scope of this experiment by varying the friction force and observing its relationship with mass sensitivity and transmissibility.

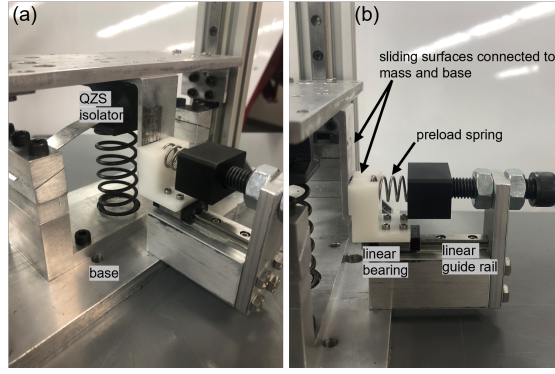


Figure 3: Images of mechanism built for precisely controlling the friction force between the mass and base: isometric view (a), and side view (b).

The experimental protocol was conducted step by step as follows:

1. The preload screw was turned to apply an incremental normal force to the sliding surfaces
2. Static testing of the isolator was performed for loading and unloading directions to determine the hysteresis magnitude
3. Without adjusting the preload, the isolator was moved to the shaker for dynamic testing
4. Vibration testing was done with weights varying between underloaded, ideal, and overloaded. The ideal weight was assumed to be the average of the loading and unloading curves in the QZS region
5. Static testing was repeated to confirm force-deflection behavior had not changed
6. Steps 1-5 were repeated for the next hysteresis level

Four different hysteresis levels and five different weights at each level were tested for a total of 20 data sets. The vibration testing setup is pictured in Figure 4. The base motion was controlled by VibrationView software, and constant displacement sine sweeps were performed. The displacement was 1.25 mm peak to peak and the sweep rate was 10 Hz/min. Accelerometers were mounted on the base and mass to record the input and output respectively.

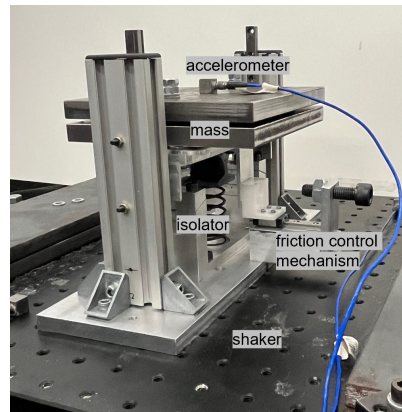


Figure 4: Setup of QZS isolation system on the shaker for base excitation testing

4. RESULTS AND DISCUSSION

4.1. Static and Dynamic Testing to Evaluate Hysteresis and Weight Sensitivity

The measured force-deflection curve of the isolator without addition of friction is plotted in Figure 5a. The hysteresis in the QZS region is approximately 1 N, and we expect that this can be attributed primarily to friction in the linear guide rail system. This was confirmed by measuring the force-deflection without the guide rails attached, and no detectable hysteresis was present.

For the purposes of this study, we defined the ideal weight as the average force between the loading and unloading curves in the middle of the QZS region (at a displacement of 8.5 mm). It is important to mention that despite this definition, it is possible that the experimental data may show that a different weight results in lower transmissibility. The weight was varied by -5% to $+5\%$ deviation from this ideal weight in increments of 2.5% . The exact values corresponding to -5.0 , -2.5 , 0.0 , $+2.5$, and $+5.0$ percent deviation were 43.6 , 44.8 , 46.0 , 47.1 , and 48.3 N respectively and are shown as horizontal dashed lines on Figures 5a-d. It is seen that the friction force can be effectively controlled to give hysteresis of 1 , 3 , 5 and 7 N as shown.

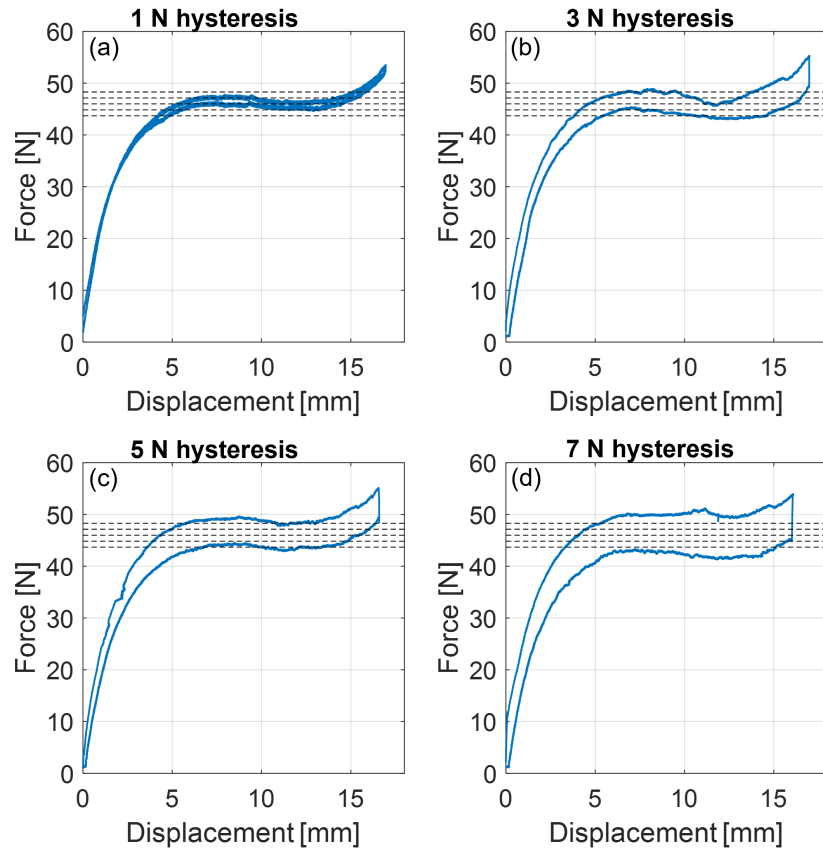


Figure 5: Experimental force-deflection results of QZS isolator with varying hysteresis magnitude

Each of these configurations was subject to base excitation, and the transmissibility results are plotted in Figure 6. The results confirm our hypothesis that increasing hysteresis reduces the weight sensitivity but also reduces the isolation performance. When the hysteresis is 1 N, the performance at

both low and high frequencies becomes worse when the weight is not ideal. However, it is interesting that the 44.8 N weight (-2.5% variation) results in the best performance. This could be explained by the fact that the QZS region in Figure 5a actually contains a slightly negative slope which obscures the determination of the ideal weight.

At 3 N hysteresis a significant reduction in sensitivity is already achieved, and the transmissibility becomes decreasingly weight sensitive as hysteresis increases to 5 N and 7 N. However, a flat response also develops at low frequency, and the transmissibility does not become zero until higher frequencies as hysteresis increases. Transmissibility at low frequencies appears to be performance aspect most affected by the tradeoff. The isolator with 3 N hysteresis arguably has a good balance between performance and low weight sensitivity. It has no resonances and transmissibilities which do not go above 1.5 dB for any weight variation.

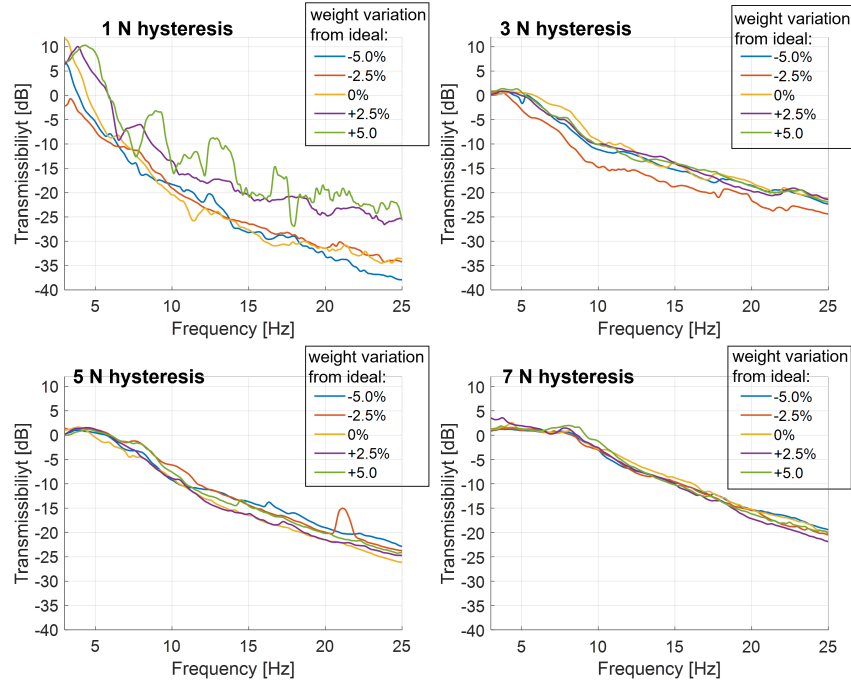


Figure 6: Transmissibilities for all variations of hysteresis and weight determined from experimental base excitation testing.

The base excitation system was simulated using Equation 1. The model results in Figure 7 agree well with the experimental data and accurately show that the isolator is highly weight sensitive with 1 N hysteresis and less sensitive with higher hysteresis. The transmissibility magnitudes are also close to the experimental values across all frequencies.

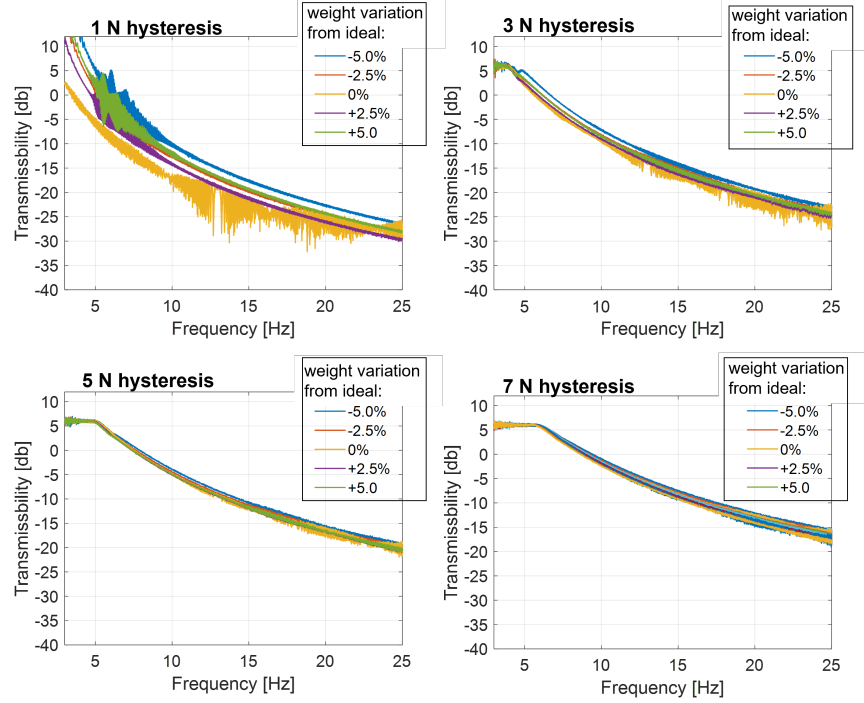


Figure 7: Model results for transmissibility of QZS isolator with different hysteresis and weights

4.2. Futher Improvement of QZS Isolator

An important question arising from the vibration testing results is how to further improve the isolator performance. For example, it may be desirable to have negative transmissibilites starting in the 1-3 Hz range. Since the model was validated with the experimental results, we used it to investigate which parameters can be optimized to further improve the performance. We found that the two important parameters for reducing the transmissibility between 1 and 5 Hz were the slope in the QZS region and the hysteresis. In particular, it is important for the slope in the QZS region to be exactly zero and for the hysteresis to be as low as possible while being matched with the ideal weight. If all these conditions are met, the isolation performane at low frequency can be significantly improved. In practical applications, it is difficult to achieve exactly zero slope in the QZS region (as evidenced from the slightly negative slope in Figure 5). This is due to the high sensitivity of the spring steel arch negative stiffness to the geometry and assembly. Very small variations in the post-buckled length and thickness can easily alter the force-deflection characteristic. It is also difficult to completely eliminate hysteresis in practical devices. These are two challenges of QZS isolators to consider in future work.

4.3. Method to Adjust QZS Force

Considering the previous discussion on performance tradeoff and further improvement, a method to adjust the QZS force in-situ while maintaining low hysteresis would be greatly beneficial. This is one of the major barries of QZS isolators toward practical applications, yet few solutions have been proposed in the literature. Furthermore, to our surprise, we found that a very simple and effective solution exists for certain types of QZS isolators.

As shown in Figure 8a, the flat force can be programmed by simple preloading of the linear spring. It is seen that this solution can not only adjust for weight changes of a few percent but also much

larger variations up to 50%. Figure 8b shows that the flat force is approximatley linear with the preload, which is advantageous for control purposes. It is expected that this control strategy can be used semi-actively or even actively to optimize the isolator performance.

If the arch is in its original, unloaded position, and a vertical preload force pushes upward on the arch at its center, it will have negligible upward displacement. In other words, the stiffness of the arch is significantly higher in the upward direction than in the downward direction, which allows this adjustment concept to work. As a result, when weight is applied, the arch has the same starting position and stiffness characteristics in the downward direction regardless of preload. Such adjustment is possible whenever the negative stiffness element has a similar characteristic, and disc springs are one example. To our knowledge, this is the first QZS isolator to have true force tunability without high complexity or staircase-type behavior which has limited practical utility.

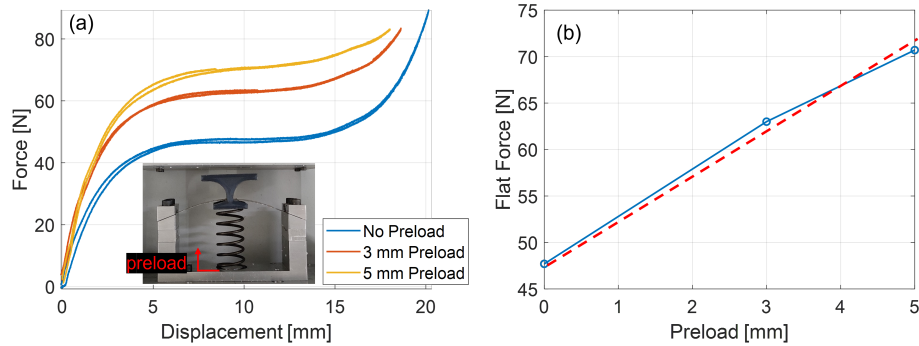


Figure 8: Adjusting the QZS force by preloading the linear spring: Force-deflection curves for different preload (a), and relationship between QZS force and preload (b).

5. CONCLUSIONS

The goal of this paper was to experimentally investigate the tradeoff between performance and weight sensivity of QZS isolators, which is dictated by the hysteresis in the QZS region. A QZS isolator based on a compression spring and prestressed spring steel arch was designed and fabricated. A mechanism to controllably apply different friction forces in a base excitation system was incorporated into the QZS isolator. The experimental results confirmed the hypothesis that the isolator has the best performance when hysteresis is low but also the largest weight sensitivity. The equation of motion of the system was solved numerically to validate the experimental results, and then the model was used to investigate possible improvements to the isolator. Lasly, a simple method to shift the QZS foce in-situ was demonstrated, which is expected to enable a wider range of practical applications by overcoming the tradeoff.

REFERENCES

- [1] Chaoran Liu, Kaiping Yu, Baopeng Liao, and Rongping Hu. Enhanced vibration isolation performance of quasi-zero-stiffness isolator by introducing tunable nonlinear inerter. *Communications in Nonlinear Science and Numerical Simulation*, 95:105654, 2021.

- [2] RA Ibrahim. Recent advances in nonlinear passive vibration isolators. *Journal of sound and vibration*, 314(3-5):371–452, 2008.
- [3] A Carrella, MJ Brennan, and TP Waters. Static analysis of a passive vibration isolator with quasi-zero-stiffness characteristic. *Journal of sound and vibration*, 301(3-5):678–689, 2007.
- [4] Junhan An, Guoping Chen, Xi Deng, Chen Xi, Tao Wang, and Huan He. Analytical study of a pneumatic quasi-zero-stiffness isolator with mistuned mass. *Nonlinear Dynamics*, 108(4):3297–3312, 2022.
- [5] Ali Abolfathi, Michael John Brennan, TP Waters, and Bin Tang. On the effects of mistuning a force-excited system containing a quasi-zero-stiffness vibration isolator. *Journal of Vibration and Acoustics*, 137(4), 2015.
- [6] Yong Wang, Shunming Li, Xingxing Jiang, and Chun Cheng. Resonance and performance analysis of a harmonically forced quasi-zero-stiffness vibration isolator considering the effect of mistuned mass. *J. Vib. Eng. Technol*, 5(1):45–60, 2017.
- [7] Akintoye Olumide Oyelade. Vibration isolation using a bar and an euler beam as negative stiffness for vehicle seat comfort. *Advances in Mechanical Engineering*, 11(7):1687814019860983, 2019.
- [8] Xiuchang Huang, Xingtian Liu, Jingya Sun, Zhiyi Zhang, and Hongxing Hua. Vibration isolation characteristics of a nonlinear isolator using euler buckled beam as negative stiffness corrector: a theoretical and experimental study. *Journal of Sound and Vibration*, 333(4):1132–1148, 2014.
- [9] Srajan Dalela, PS Balaji, and DP Jena. Design of a metastructure for vibration isolation with quasi-zero-stiffness characteristics using bistable curved beam. *Nonlinear Dynamics*, 108(3):1931–1971, 2022.
- [10] Xiuchang Huang, Yong Chen, Hongxing Hua, Xingtian Liu, and Zhiyi Zhang. Shock isolation performance of a nonlinear isolator using euler buckled beam as negative stiffness corrector: Theoretical and experimental study. *Journal of Sound and Vibration*, 345:178–196, 2015.
- [11] Zhongwen Zhang, Fenglan Shi, Chuang Yang, and Zhao-Dong Xu. Quasi-zero stiffness isolator based on bistable structures with variable cross-section. *Journal of Low Frequency Noise, Vibration and Active Control*, 41(1):405–416, 2022.
- [12] Wenzhong Yan, Yunchen Yu, and Ankur Mehta. Analytical modeling for rapid design of bistable buckled beams. *Theoretical and Applied Mechanics Letters*, 9(4):264–272, 2019.
- [13] Safvan Palathingal and GK Ananthasuresh. Design of bistable arches by determining critical points in the force-displacement characteristic. *Mechanism and Machine Theory*, 117:175–188, 2017.
- [14] Ge Yan, Zhi-Yuan Wu, Xin-Sheng Wei, Sen Wang, Hong-Xiang Zou, Lin-Chuan Zhao, Wen-Hao Qi, and Wen-Ming Zhang. Nonlinear compensation method for quasi-zero stiffness vibration isolation. *Journal of Sound and Vibration*, 523:116743, 2022.
- [15] Xingtian Liu, Qiang Zhao, Zhiyi Zhang, and Xubin Zhou. An experiment investigation on the effect of coulomb friction on the displacement transmissibility of a quasi-zero stiffness isolator. *Journal of Mechanical Science and Technology*, 33:121–127, 2019.